

# Image processing approach to determine the severity level of tuberculosis

## ABSTRACT

Tuberculosis (TB) is a disease caused by a bacterium called ***Mycobacterium tuberculosis***. Basically there are two types of TB, latent and pulmonary TB. Its symptoms include persistent cough for more than two weeks, cough with blood, night sweat, tiredness, fever, chest pain, lymph node enlargement. Its treatment depends on severity level such as mild, moderate, severe and very severe and this can be obtained from TB diagnosis such as chest x-ray image, nucleic acid amplification test and culture and sensitivity. The main aim of this work is to determine severity level of TB using image processing techniques. Chest x-ray (CXR) images of TB patients were obtained from Google image. Firstly, the CXR images were enhanced from Red Green Blue (RGB) to gray image (GI) form. Secondly, GI were decomposed, convolved, compressed and filtered these processing is called image degradation. Thirdly, These GI were restored and binarized. a threshold value  $\geq 53$  was obtained to classify the severity level of the infected image. Furthermore, average error was calculated and system performance obtained. This work revealed that image 1, 2, 6 and 11 has a total pixel value 11067, 6735, 9256 and 3894 respectively  $\geq 53$  which indicates that the % of the infected areas as 99.62%, 99.52%, 96.70% and 82.78% respectively which shows the severity level are very severe. While the image 3, 4, 5, 8 and 9 has a percentage of infected areas 73.13%, 72.90%, 76.80%, and 76.84% respectively which indicate the severity level as severe. Image 7 has a percentage of infected area 51.21 which shows the severity level as moderate. This research work revealed that image processing is a suitable technique for determine the severity level of TB.

**Keywords:** Tuberculosis, Mycobacterium Tuberculosis, Image processing, severity level, X-ray, culture and sensitivity.

## 1. Introduction

Tuberculosis (TB) is a contagious disease caused by bacteria called Mycobacterium Tuberculosis [1]. According to [2] Tuberculosis is the second leading killer disease from an infectious disease worldwide, after the Human Immune deficiency Virus (HIV). Basically, there are two main types of TB infections; Latent and Active TB, in latent TB the bacteria remain in an inactive state but there are 10% chances of latent TB becoming active TB. However people with HIV are more prone to TB infection. The typical indicators of active pulmonary TB are persistent cough for more than two weeks, cough with blood, fever, Night sweat, tiredness, and lymph node enlargement [3]. In the context of medicine, mild (M), moderate (M), severe (S) and very severe (VS) are the major yardstick for measuring the severity level of the diseases, Chest radiography is one of the most important way of screening and determining the severity level of TB. Image processing techniques in recently applied to many research areas such as security, engineering, forensic science, Material science, Medical diagnosis and film industries among others. Image

37 processing combine with computer algorithms to enhance, Restore, filter, classify, compress,  
38 segment, or threshold in order to obtain necessary information and draw conclusion or make  
39 decision [3].

40 Some other techniques in computational intelligence are applied in medical diagnosis, prognosis  
41 and determining the severity level of the disease for example genetic programming was used to  
42 detect diabetes in [5]. Pulmonary tuberculosis was diagnosed using artificial neural network in  
43 [6]. Fuzzy inference system was applied to predict risk level in [7]. In the work of [8] Fuzzy  
44 Logic based Health Care System using Wireless Body Area Network was implement. Generic  
45 Medical Fuzzy Expert System for Diagnosis of Cardiac Diseases was implemented in [9]. In [10]  
46 they uses two image processing techniques repetitive smoothing-sharpening and ridge detection  
47 algorithm to diagnose the early stage of TB and the results was tested on lung X-ray image which  
48 enhance the image contrast for easy classification of TB. [11] conducted texture analysis on TB  
49 X-ray images using image processing techniques 49 images were used for the experiment to  
50 measure the 1<sup>st</sup> and 2<sup>nd</sup> order texture features. Image processing techniques (image enhancement,  
51 segmentation and feature extraction) has been applied in [12] for the detection of lung cancer.  
52 Support Vector machine approach was used in [13] for detecting and counting the number of TB  
53 bacteria from Microscopic imaging. [14] Developed CXR tuberculosis detection using image  
54 processing techniques. [15] Introduced the concept, sign and symptom of brain tumor and also  
55 provide an overview on the various method and algorithm use to detect brain tumor such as  
56 image processing, image enhancement, image segmentation and classification. [16] Presented a  
57 method for automatic identification of TB using segmentation and post processing techniques and  
58 they obtained the overall sensitivity level at 96.80% and the error rate at 3.38%. [17] provide an  
59 overview of publications between 1998 and 2014 on the automatic diagnosis of TB and the  
60 review proved that the algorithms used for this diagnosis and detection significantly increased  
61 year by year. Digital image processing techniques were presented in [18] for TB screening, lungs  
62 region were extracted using K-means segmentation.

63 Fuzzy C-means algorithm and Adaptive Neuro-fuzzy were proposed in [19] to diagnoses diabetes  
64 with the reduction of fuzzy rules with small number of linguistic variables and they have obtained  
65 CC= 83.85%, Se = 82.05% and 86.23% based on their comparison with other cases. Genetic  
66 programming methodology has applied in [20] for detection of diabetes. Stepwise Classification

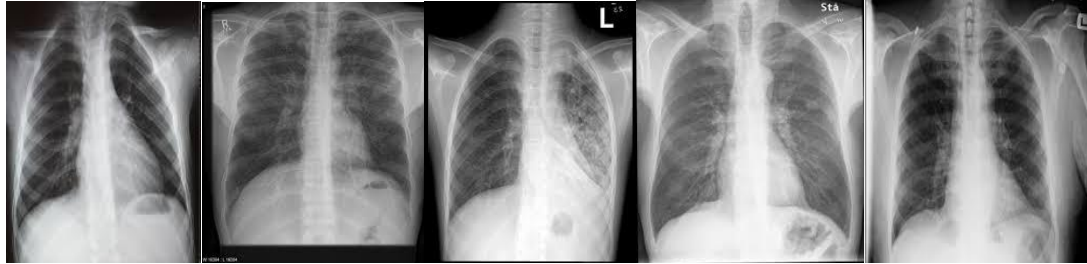
67 algorithm was developed in [21] for detecting and counting the number of TB bacteria. Adaptive  
68 Neuro-fuzzy was applied to medical imaging in [22] to detect and recognize brain tumor. Neuro-  
69 fuzzy system was used in [23] to classify electrocardiogram (ECG) for Heart rate Variability  
70 (HRV). [24] developed a system that would determine the severity level of osteomyelitis using  
71 Adaptive Neuro-fuzzy model. [25] Applied Neuro-fuzzy approach to diagnosis TB and control  
72 where they used symptoms of TB yield good results.

73 The main aim of this research work is to determine the severity level of TB using Image  
74 processing technique and this can be achieve by addressing the following challenges; To enhance  
75 the CXR images collected, To degrade the images and covert them from Red Green Blue (RGB)  
76 to gray images, To restore the images and binarize them cut the threshold value and to calculate  
77 the error and performance of the model.

## 78 2. METHOD OF DATA COLLECTIONS

79 Chest X-ray images of TB patients were collected from  
80 [https://www.google.com/search?q=TB+Xray+images&dcr=0&source=lnms&tbn=isch&sa=X&ved=0ahUKEwjEqrKQx\\_TZAhVC6aQKHRxeCLcQ\\_AUICigB&biw=1525&bih=741](https://www.google.com/search?q=TB+Xray+images&dcr=0&source=lnms&tbn=isch&sa=X&ved=0ahUKEwjEqrKQx_TZAhVC6aQKHRxeCLcQ_AUICigB&biw=1525&bih=741) the images  
81 were cropped to get the exact region of interest of which all of them are 161x161 dimension,  
82 which form our image datasets. The images were converted from RGB color map to Gray scale  
83 color map. Then these images are read one by one to the workspace and display their Histogram  
84 equalization to see the intensity levels of every image and the number of pixels which is used to  
85 judge the severity level of patients. Team of medical expertise was interviewed to indicate the  
86 severity level by circling the infected areas on the images state the severity level of the image  
87 either mild, moderate severe and very severe. We have then used image processing techniques to  
88 make judgment also either mild moderate severe and very severe. The two results were compare  
89 and contrast to arrive at conclusion. The data collected were presented in the Figure 1.a - k;

91



92  
93

Figure 1a

Figure 1b

Figure 1c

Figure 1d

Figure 1e



94  
95

Figure 1f

Figure 1g

Figure 1h

Figure 1i

Figure 1j



96  
97

Figure 1k

98  
99

### 3. METHOD OF DATA ANALYSIS

100 Cameras and x-ray images usually contain periodic noise or electromechanical interference  
 101 during the image acquisition. In medical diagnosis, if the information supplied to the medical  
 102 experts is inadequate, wrong treatment may be offered to the patient which in return may led to  
 103 increase in the severity level of the disease or triggers different illness. Therefore, to guarantee  
 104 correct medical treatment, adequate medical information should be provided to the medical  
 105 expertise especially, in TB treatment information about all infected areas have to be cleared and  
 106 this can be done using digital image processing (DIP). In the DIP chest x-ray (CXR) images need  
 107 to be enhanced, degraded and restored.

#### 108 3.1 IMAGE ENHANCEMENT

109 Image enhancement involves the conversion of CXR image in red green blue (RGB) form to gray  
 110 image. This can be done to determine basic information about CXR image. In this work, model of  
 111 expression (1) is applied to convert the CXR image to gray form.

112 
$$g(x, y) = 0.299 \times R + 0.587 \times G + 0.114 \times B \quad (1)$$

113 Where  $x$  and  $y$  are image dimensions, then the gray image is further degraded.

### 114 3.2.IMAGE DEGRADATION

115 Image degradation involves decomposition, convolution, compression and filtering. In this work,  
116 the degradation function  $f(x, y)$  and noise term operate as inputs, is given by

117 
$$g(x, y) = H[f(x, y) + Z(x, y)] \quad (2)$$

118 Where  $f(x, y)$  gives the image intensity position at  $(x, y)$  and is the operator that provides  
119 knowledge about the degradation function and  $Z(x, y)$  gives the knowledge about the noise  
120 terms. It is believed that, when  $H$  and  $Z$  are properly chosen, information about the CXR may  
121 be closer to the original. In other words, if  $H$  and  $Z$  are linear then the spatial invariants are seen  
122 clearly and the image degraded in the spatial domain is given by (3)

123 
$$g(x, y) = h(x, y) \times f(x, y) + z(x, y) \quad (3)$$

124 Where  $h(x, y)$  is the spatial representation of the degradation function and “ $\times$ ” indicates the  
125 convolution. However, the multiplication in frequency domain forms what is called Fourier  
126 information pair and its Fourier corresponding model in equivalent frequency domain is  
127 expressed in (4).

128 
$$G(u, v) = H(u, v)F(u, v) + N(u, v) \quad (4)$$

129 Where  $H, F$  and  $N$  are the Fourier transforms that correspond to the terms in (3) which forms the  
130 degradation model.

131 Furthermore, the degraded image is compressed using (5) to reduce the number of bits required in  
132 presenting the image

133 
$$g(x, y) = f(x, y) + \frac{1}{N} \sum_{k=i}^n n_k(x, y) \quad (5)$$

134 The compressed image is filtered to remove all the unwanted terms (noise). In fact, it is important  
135 to note that, attention must be given to the choice of right filter, this because information about  
136 the image at that time is not cleared, since the image is compressed. In this work, Butterworth

137 notch filter is chosen because the major possible approach to filter noise components is via notch  
 138 filtering, since periodic noise manifest itself and becomes visible in Fourier spectrum. The filter  
 139 model is given in (6)

$$140 \quad H(u, v) = \frac{1}{1+[D_0^2+D_1(u,v)D_2(u,v)]^n} \quad (6)$$

$$141 \quad D_1(u, v) = \left[ \left( u - \frac{m}{2} - U_0 \right)^2 + \left( v - \frac{N}{2} - V_0 \right)^2 \right]^{1/2} \quad (7)$$

$$142 \quad D_2(u, v) = \left[ \left( U - \frac{m}{2} + U_0 \right) \right]^{1/2} \quad (8)$$

143 Where  $(U_0, V_0)$  and  $(-V_0 - U_0)$  are the locations and the notation  $D_0$  is their radius.

144 After successful filtering the CXR image needs to be restored.

### 145 **3.3.RESTORATION OF CXR**

146 The simplest approach to restore a degraded image is to form an estimate of a form

$$147 \quad \hat{F}(u, v) = \frac{G(u,v)}{H(u,v)} \quad (9)$$

148 Usually Fourier transform of  $G(u, v)$  and  $H(u, v)$  takes the degraded CXR image. So, the inverse  
 149 filtering model can be obtained as

$$150 \quad \hat{F}(u, v) = F(u, v) + \frac{N(u,v)}{H(u,v)} \quad (10)$$

151 The ratio  $\hat{F}(u, v) = \frac{G(u,v)}{H(u,v)}$  gives limit to the frequency range i.e. near the original. The idea is  
 152 that zero's in  $H(u, v)$  are less likely to occur near the original CXR image because the intensity of  
 153 transform is typically at the peak value is that region. In a broad sense, special treatment is given  
 154 to  $(u, v)$  for which  $H$  is zero or near zero. In some cases, after the inverse filtering Wiener filter  
 155 may be applied to further filter the remaining noise components, which in this case is not applied.

156 Therefore, the statistical error function is estimated using (11)

$$157 \quad E^2 E[(f - \hat{F})^2] \quad (11)$$

158 Where  $E$  is the expected value operator,  $f$  is the ungraded CXR image and  $\hat{F}$  is the  
159 restored CXR image and the restored image becomes

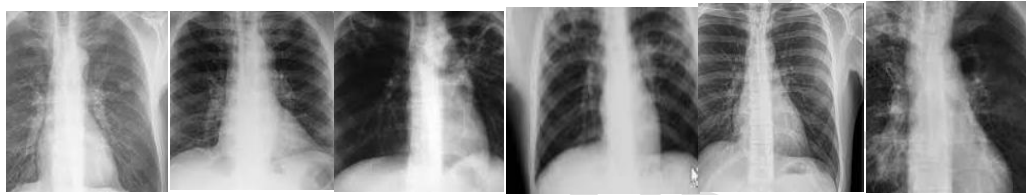
$$160 \quad g(x, y) = \hat{F}(x, y) \quad (12)$$

161 The performance of the DIP is given by

$$162 \quad \Delta = (100 - e)\% \quad (13)$$

#### 163 4. RESULTS

164 Figure 2(a-k) present the final restored images, and Table 1 shows the restored images in terms  
165 of pixel values.



166  
167 Fig. 2a Fig. 2b Fig. 2c Fig. 2d Fig. 2e Fig. 2f



168  
169 Fig. 2g Fig. 2h Fig. 2i Fig. 2j Fig. 2k

**Table 1** Image information analysis

Image	$F$	$\hat{F}$	$e$	infected pixel $\geq 53$	% of the infected area
Image 1	11250	11109	141	11067	99.62%
Image 2	9414	9300	114	9256	99.52%
Image 3	7918	7866	52	5753	73.13%
Image 4	8790	8710	80	6908	79.31 %
Image 5	7821	7705	116	6162	79.97%
Image 6	7172	6954	218	6735	96.71%
Image 7	9371	9304	67	4765	51.21%
Image 8	5521	5406	115	3941	72.92%
Image 9	6411	6367	44	4890	76.80%
Image 10	6412	6380	32	4903	76.84%
Image 11	4815	4704	111	3894	82.78%

### Difference between $F$ and $\hat{F}$

The Fig. 3 represents the raw images ( $F$ ) and the processed ( $\hat{F}$ ), the number of pixels in the raw images are higher than the number of pixels in the processed images, that is noised are removed during the processing. The red line indicates the raw images and the blue line indicates the processed images, the Y axis represents the number of pixels and X axis represent the images. In image 1 the number of pixels are 11250 while the processed image has 11109 pixels making the difference of 141 and so on.

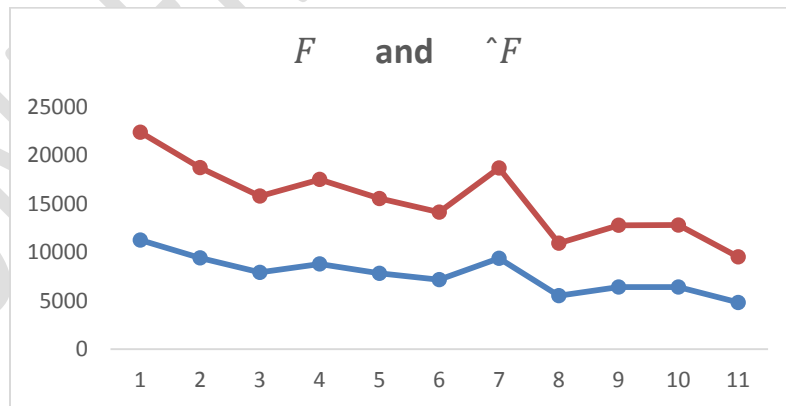


**Figure 3** The difference between  $F$  and  $\hat{F}$

The severity level of the disease is measure using mild, moderate, severe and very severe as indicated in the work of [24], in this work from Fig. 4 image 1 has a severity level as very severe



(99.62%), follow by image 2 which has 99.52%, and image 6 also has 96.71%, However, image 7 has 51.21% and so on.

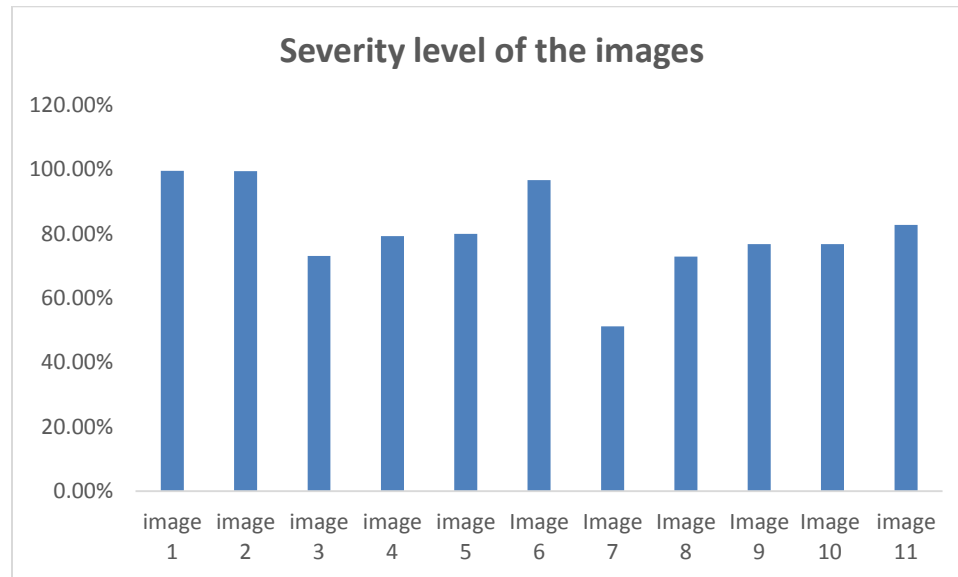


**Figure 4** Severity level of the images

## 5. DISCUSSION

From table 1. processed images ( $\hat{F}$ ) 1, 2, 6 and 11 has a total pixel values 11067, 6735, 9256 and 3894 respectively  $\geq 53$  which indicates the percentage of the infected areas are 99.62%, 99.52%, 96.70% and 82.78% respectively which shows the severity level are very severe. While the image 3, 4, 5, 8 and 9 respectively has a percentage of infected areas 73.13%, 72.90%, 76.80%, and 76.84% respectively which indicate the severity level as severe. Image 7 has a percentage of infected area 51.21% which shows the severity level is moderate. Furthermore Fig. 3 depict the differences between the raw images ( $F$ ) and the processed images ( $\hat{F}$ ) which also shows that raw images has noised. Finally Fig. 4 indicates the severity level of all the images in terms of percentages.

## 6. CONCLUSION

In this research work image processing techniques are applied to determine the severity level of Tuberculosis. This research work pave away and proved that image processing is suitable techniques would be applied to medical diagnosis especially disease that require medical images in diagnosis.

## Reference

- [1] National Jewish Health. Causes of Tuberculosis, <https://www.nationaljewish.org/conditions/tuberculosis-tb/causes>; 2013 [accessed 3<sup>rd</sup> March, 2017].
- [2] Mahmoud RS, Shahaboddin S, Shahram G, Teh Y, Aghabozorgi S, Laiha M, Valentina E, *et al.*, RAIRS2 A new expert system for diagnosing Tuberculosis with real world tournament selection mechanism inside artificial immune recognition system *Int. Fed. for Med. and Bio. Engr.* 2015; 15:1323-6
- [3] Navneet W, Sharad KT and Rahul M, Design and identification of tuberculosis using fuzzy based decision support system *Adv. in Comp. Sci. and Inf. Tech.* 2015; 2: 57-62
- [4] Kamble PA Anagire VV and Chamtagoudar NS CXR tuberculosis detection using MATLAB *Im. Proc. Int. Res. J. of Engr. and Tech.*, 3: 2342-4
- [5] Pradhan *et al.*, (2012) A Genetic Programming Approach for Detection of Diabetes *International Journal of Computational Engineering Research* 2(6) pp.91-94
- [6] Chandrika V., Parvathi C.S. and P. Bhaskar, (2012). Diagnosis of Tuberculosis Using MATLAB Based Artificial Neural Network *IJIPA*: 3(1): 37-42
- [7] Ekong V. E., Uyinomen O., Uwadiae, Enobakhare E., Abasiubong, Festus, Onibere & Emmanuel A. (2013) A Fuzzy Inference system for predicting depression risk levels *African Journal of mathematics and computer Science Research*, 6 (10), 197-204.
- [8] Prakashgoud P. & Samina M. (2013). Fuzzy Logic based Health Care System using Wireless Body Area Network *International Journal of Computer Applications* Vol. 80 (13) pp. 46-51.
- [9] Smita S.S., Sushil S., M. Ali S. 2013. Generic medical fuzzy expert system for diagnosis of cardiac diseases *International Journal of Computer Application* 66(13), 35-44.
- [10] Chandrika V., Parvathi C.S., and P. Bhaskar 2012. Multi-level Image Enhancement for Pulmonary Tuberculosis Analysis *International Journal of Science and Applied Information Technology* 1(4):102-106
- [11] Patil S. A. 2012 Texture Analysis of TB X-Ray Images Using Image Processing Techniques *Journal of Biomedical and Bioengineering*, 3(1): 53-56.
- [12] Mokhled S. A. T. 2012. Lung Cancer Detection Using Image Processing Techniques *Leonardo Electronic Journal of Practices and Technologies* 147-158
- [13] Kusworo A., Rahmad G., Aris S., K. Sofjan F., Adi P., Ari B. 2013. Tuberculosis (TB) Identification in the Ziehl-Neelsen Sputum Sample in NTSC Channel and Support Vector Machine (SVM) Classification *International Journal of Innovative Research in Science, Engineering and Technology* 2(9): 5030-5035

- [14] Kamble P. A. Anagire V. V. & Chamtagoudar N. S. 2016. CXR Tuberculosis Detection Using MATLAB *Image Processing International Research Journal of Engineering and Technology* 3(6):2342-2344
- [15] Rohan K. G., Savita A. L. & Santosh G. V. 2016. Identification of Brain Tumor using Image Processing Technique: Overviews of Methods *SSRG International Journal of Computer Science and Engineering* 3: 89-93
- [16] Cicero F. F. C. F., Pamela C., Clahildek M. X., Luciana B. M. F., Marly & Guimarães F. C. 2015 Automatic identification of Tuberculosis mycobacterium *Research on Biomedical Engineering* 31(1):33-43
- [17] Panicker R.O., Soman B., Saini G. and Rajan J. 2016. A Review of Automatic Methods Based on Image Processing Techniques for Tuberculosis Detection from Microscopic Sputum Smear Images *Journal of Medical system* 40(1)
- [18] Chetarn C. P. and Ganorkar S. R., 2016. Tuberculosis Screening Using Digital Image Processing Techniques *International Research Journal of Engineering and Technology* 3(1): 623-627
- [19] Nesma S., Meryem S. and Mohamed A.C. 2012. Interpretable Classifier of Diabetes Disease *International Journal of Computer Theory and Engineering*, 4(3):438-442
- [20] Pradhan M. A., Bamnote G. R., Vinit T., Kiran J., Vijay C. and Vijay D. 2012. A Genetic Programming Approach for Detection of Diabetes *International Journal of Computational Engineering Research* 2(6):91-94
- [21] Ajay D., Corina P., Gerrit C., Tarlochan S., Fleming Y. M. L. and Sean K. 2012. Automated Detection of Tuberculosis on Sputum Smear Slides using Stepwise Classification *Proceeding SPIE Medical Imaging Conference (8315-123), Newport Beach, CA, Feb 4 – 9, 2012*
- [22] Anant B. and Kapil K. S. 2013. An Approach to Medical Image Classification Using Neuro Fuzzy Logic and ANFIS Classifier *International Journal of Computer Trends and Technology* 4(3):236-240
- [23] Hoang C., Thuan N. and Trung L. (2013) Neuro-Fuzzy Approach to Heart Rate Variability Analysis *International Journal of Bioscience, Biochemistry and Bioinformatics*, 3(5):456-459
- [24] Jerome M. G., Ibrahim Goni and Timothy U. M. 2017. Adaptive Neuro-fuzzy system for Determining the severity level of osteomyelitis and control, *Archives of Applied Science Research*, 9 (2):9-15.
- [25] Jerome M. G., Ibrahim Goni & Mohammed Isa 2018. Neuro-Fuzzy Approach for Diagnosing and Control of Tuberculosis *the International Journal of Computational Science, Information Technology and Control Engineering* 5(1)

UNDER PEER REVIEW